FOR FURTHER

(12)

A Foliage Penetration Summary

AUGUST GOLDEN, Capt, USAF

D D C

JUN 20 1978

F

ROME AIR DEVELOPMENT CENTER
AIR FORCE SYSTEMS COMMAND
GRIFFISS AIR FORCE BASE, NEW YORK 13441

AD No.
DDC FILE COPY

AD A055391

Best Available Copy 78 06 09 057

This report has been reviewed by the RADC Information office (OI)
and is releasable to the National Technical Service (NTIS). At NTIS
it will be releasable to the general public, including foreign nations.

This technical report has been reviewed and approved for publication.

APPROVED:

PHILIPP BLACKSMITH
Chief, Electromagnetic Systems Concepts Branch

APPROVED:

WALTER ROTMAN
Acting Chief
Electromagnetic Sciences Division

FOR THE COMMANDER:

Plans Office

REPORT DOCUMENTATION PAGE		READ INSTRUCTIONS BEFORE COMPLETING FORM
1. REPORT NUMBER RADC-TR-78-34	2. GOVT ACCESSION NO.	3. RECIPIENT'S CATALOG NUMBER
4. TITLE (and Subtitle) A FOLIAGE PENETRATION SUMMARY		5. TYPE OF REPORT & PERIOD COVERED In House
		6. PERFORMING ORG. REPORT NUMBER
7. AUTHOR(s) August Golden, Capt, USAF		8. CONTRACT OR GRANT NUMBER(s)
9. PERFORMING ORGANIZATION NAME AND ADDRESS Deputy for Electronic Technology (RADC/EEC) Hanscom AFB Massachusetts 01731		10. PROGRAM ELEMENT, PROJECT, TASK AREA & WORK UNIT NUMBERS 46001502 PE62702F
11. CONTROLLING OFFICE NAME AND ADDRESS Deputy for Electronic Technology (RADC/EEC) Hanscom AFB Massachusetts 01731		12. REPORT DATE February 1978
		13. NUMBER OF PAGES 27p.
14. MONITORING AGENCY NAME & ADDRESS(if different from Controlling Office)		15. SECURITY CLASS. (of this report) Unclassified
		15a. DECLASSIFICATION/DOWNGRADING SCHEDULE

16. DISTRIBUTION STATEMENT (of this Report)

Approved for public release; distribution unlimited.

17. DISTRIBUTION STATEMENT (of the abstract entered in Block 20, if different from Report)

18. SUPPLEMENTARY NOTES

19. KEY WORDS (Continue on reverse side if necessary and identify by block number)

Foliage penetration
Foliage attenuation
Radar

20. ABSTRACT (Continue on reverse side if necessary and identify by block number)

A brief survey of existing data on foliage attenuation of RF energy is presented.

It is shown that most researchers have concluded from this data that RF energy is attenuated more rapidly in foliage at higher frequencies. Also, signal reflections from the foliage/air interface are shown to be a significant loss mechanism that is relatively frequency independent. Finally, curves for predicting RF signal reflection from and attenuation within foliage are presented.

DD FORM 1473 EDITION OF 1 NOV 65 IS OBSOLETE

Contents

Illustrations

3

4

A Foliage Penetration Summary

1. INTRODUCTION

Successful airborne radar design requires the consideration of many inter-
related factors. When that radar must detect fixed and slow-moving ground targets
imbedded in a foliage environment, the factors requiring consideration increase in
number and complexity due to the increased radar performance required. Some
of these factors are the percentage of energy transmitted into the foliage region,
the attenuation of electromagnetic energy in the foliage, the target backscatter
cross-section, and the effects of multipath. We shall be concerned only with the
frequency dependence of the first two factors: the transmission of RF energy into
and its subsequent attenuation within foliage. Our approach shall be to review
existing, relevant data and theories and then to generate curves useful for the pre-
diction of system performance in foliated environments.

2. FOLIAGE ATTENUATION REVIEW

We begin by presenting existing data from various sources on the foliage
attenuation of RF energy. L. V. Surgent[1] references many sources for

1. Surgent, L. V. (1974) Foliage Penetration Radar: History and Development
Technology, Army Land Warfare Lab, Aberdeen Proving Ground, Md.

electromagnetic-field attenuation data in a report written for the Army Land Warfare Lab. Data from these sources are shown in Figure 1, which was extracted from Surgent's report. The numbers of the figure pertain to the references listed below the figure. Numbers that appear twice refer to maximum and minimum data values.

Chudleigh and Moulton[2] made a straight-line approximation for field attenuation from an essentially different set of data sources than Surgent's. Their relationship is

$$\alpha = 0.06 \, (f/100)^{0.62} \text{ dB/m} \; ; \; f \text{ in MHz} \quad .$$

Nathanson[3] summarizes the attenuation in foliage via the following approximation:

$$\alpha = 0.25 \, f^{0.75} \text{ dB/m} \; ; \; f \text{ in GHz}$$

$$= 0.044 \, (f/100)^{0.75} \text{ dB/m} \; ; \; f \text{ in MHz} \quad .$$

Nathanson references the work by Saxton and Lane that is displayed as curve 6 on Figure 1 and was one of Chudleigh's references.

Lincoln Laboratory[4] saw fit to describe the relationship between attenuation and frequency as

$$\alpha = 0.15 + 0.3 \log_{10} (f/100) \text{ dB/m} \; ; \; f \text{ in MHz}$$

$$= \log_{10} [1.412 \, (f/100)^{0.3}] \quad ,$$

which is obviously completely different from the Chudleigh or Nathanson results. Lincoln Laboratory used data from Jansky and Bailey (curve 7 of Figure 1) as part of their data in arriving at a result.

Over the frequency interval of 100 to 1000 MHz, these two formulations differ little. However, as the frequency continues to increase, a divergence in calculated attenuation develops. The Lincoln Laboratory prediction results in an attenuation proportional to the logarithm of frequency, while the other approximations indicate a variation proportional to some power of frequency less than unity.

2. Chudleigh, W., Moulton, S. (1973) Long-Range Standoff Radar Surveillance Study, AFCRL-TR-73-0145.

3. Nathanson, F.E. (1969) Radar Design Principles, McGraw Hill, p 19.

4. Lincoln Laboratory (1969) TR 472, pp 92-93.

The figure shows a log-log plot of ATTENUATION, α (db/m) on the vertical axis (0.01, 0.02, 0.05, 0.1, 0.2, 0.5) versus FREQUENCY, f (MHz) on the horizontal axis (2, 5, 10, 20, 50, 100, 200, 500, 1000, 2000) with curves labeled 5, 6, 7, 8, 9.
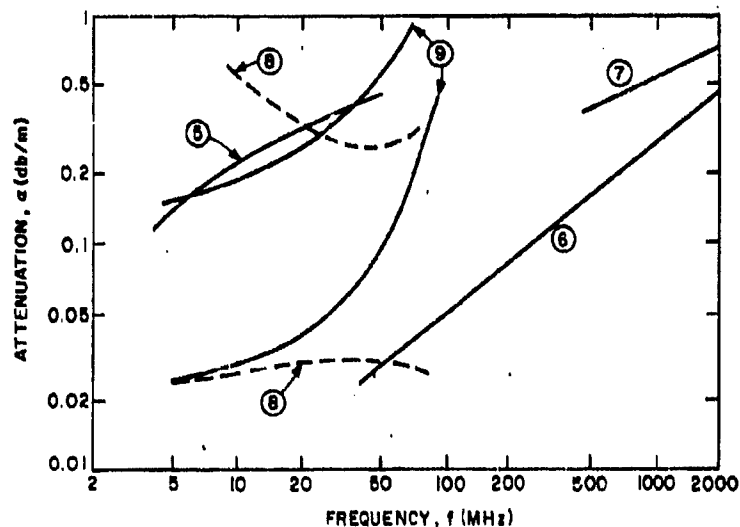
⑤ S. Krevsky, "HF and VHF Radio Wave Attenuation Through Jungle and Woods," IEEE Trans on Antennas and Propagation, Vol. AP-11, pp 506-507, July 63.

⑥ J.A. Saxton and J.A. Lane, "VHF and UHF Reception-Effects of Trees and Other Obstacles," Wireless World, Vol. 61, pp 229-232, May 1965.

⑦ L.G. Sturgill and Staff, "Tropical Propagation Research," Jansky and Bailey Engineering Dept., Atlantic Research Corp., Alexandria, VA., Final Report, Vol. 1, June 1966.

⑧ H.W. Parker and G.H. Hagan, "Feasibility Study of the Use of an Open-Wire Transmission Line, Capacitor and Cavities to Measure Electrical Properties of Vegetation," Stanford Research Inst., Special Tech Report 13, August 1966.

⑨ H.W. Parker and W. Makarabhiromya, "Electrical Constants Measured in Vegetation and in Earth at Five Sites in Thailand," Stanford Research Inst., Special Tech. Report 43, Dec 1967.

Figure 1. Foliage Attenuation vs Frequency — Averages of Measured Data

7

These various approximations to the attenuation factor are all shown in Figure 2, and it is obvious that Lincoln Laboratory is the most conservative over the frequency interval shown. This conservatism is reasonable when frequencies below 100 MHz are to be considered, due to the spread in data shown in Figure 1.

Finally, Figure 3[*] suggests that foliage-induced losses do not increase with radar operating frequencies beyond 300 MHz when the incident ray grazing angle is greater than 6 degrees.

In spite of the divergent measurements depicted on Figure 1, the preponderance of data supports the conclusion that RF signal attenuation per unit of path length increases as the frequency increases.
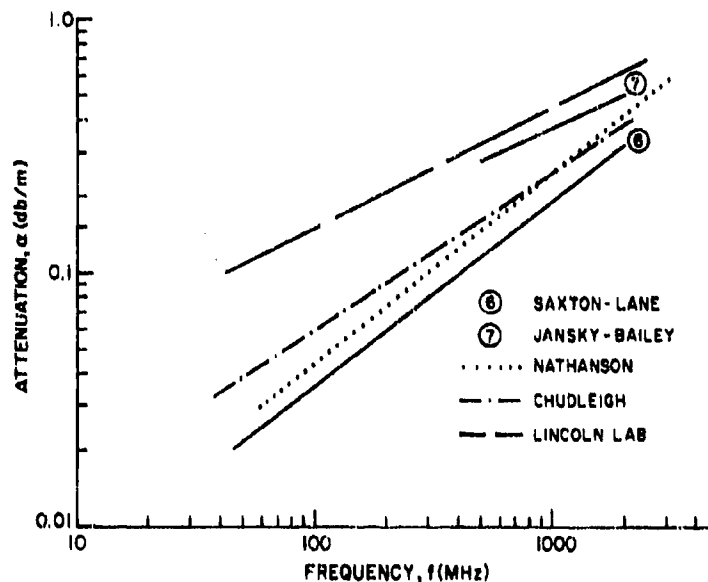

Figure 2. Foliage Attenuation vs Frequency — Plot of Various Formulations
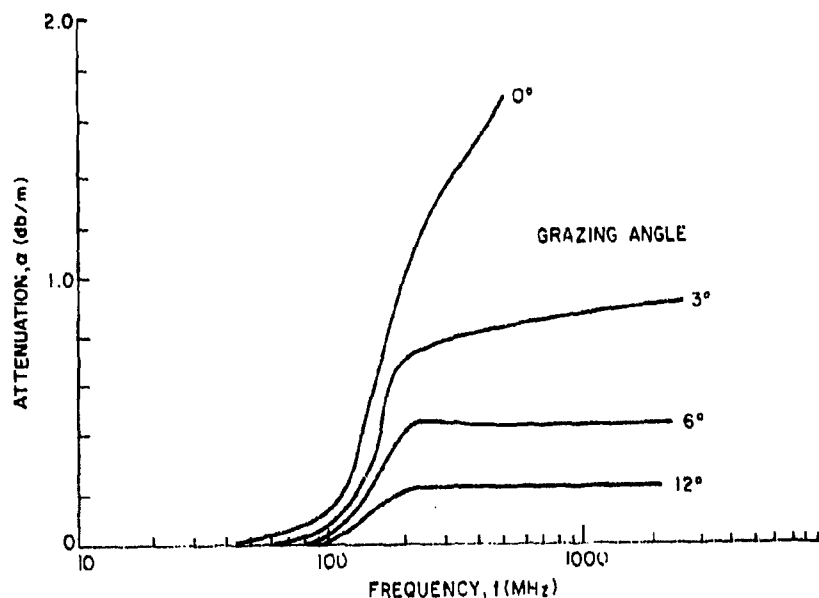

Figure 3. Foliage Attenuation vs Frequency — Multilateration Study Report

3. FOLIAGE ATTENUATION FORMULATION

How then can we explain Figure 3, which runs counter to this measured trend? Possibly through a purely mathematical development, which we shall now pursue.

Assume that a forest region, of tree height h, is a region of lossy dielectric material with a constant relative permittivity and conductivity given by ϵ' and σ respectively. According to Tamir,[5] this model may not be realistic for frequencies above 100 MHz, based on data taken by Hagn and Parker of SRI in 1960. Tamir concludes that for lower frequencies the model is good. Surgent[1] notes that the dielectric slab model for the forest has been shown to be valid for RF's up to L Band, if the model is utilized only for a "background configuration." This conclusion, Surgent indicates, results from Lincoln Laboratory's work.[6] However, we shall continue and apply this model for frequencies above 100 MHz to the problem of RF field attenuation within the slab region.

5. Tamir, T. (1967) On radio-wave propagation in forest environments, APS-15 (No. 6).

6. Lincoln Laboratory (1969) Tactical Radar Program, ESD-TR-69-354, Quarterly Progress Report.

The forest is region II of Figure 4. The incident RF energy from region I has the E field perpendicular to the plane of incidence and its propagation vector makes the angle θ_1, with the normal to the semi-infinite forest region. In this development, the finite thickness of region II is not accounted for.
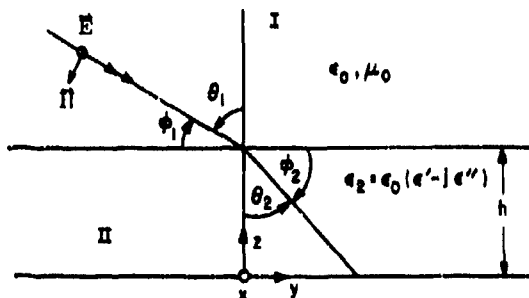
Figure 4. Problem Geometry

From Maxwells Equations, assuming $e^{j\omega t}$ time dependence in both regions, in region II we have

$$\nabla \times \vec{H}_2 = \vec{J}_2 + j\omega\epsilon \, \vec{E}_2 = (\sigma + j\omega\epsilon) \, \vec{E}_2$$

$$= j\omega\epsilon_0 \, (\epsilon' - j\epsilon'') \, \vec{E}_2$$

$$= j\omega \, \epsilon_2 \, \vec{E}_2$$

with $\epsilon'' = \sigma/\omega\epsilon_0$.

We know that the wave propagation in each region can be written as

$$\vec{E} = E_x \, \hat{x} \, e^{j\vec{k}_1 \cdot \vec{r}_1} \quad . \qquad \text{In I} \quad k_1^2 = \omega^2 \mu_0 \epsilon_0 \quad ,$$

$$\text{II} \quad k_2^2 = \omega^2 \mu_0 \epsilon_2 \quad .$$

Utilizing this complex propagation constant, we can solve for the fields in the two regions in the same manner as for lossless dielectrics, arriving at the following equations resulting from the requirement for the continuity of the electric field at the interface between regions I and II:

10

$$E_{x_1}^+ e^{-jk_1 \sin\theta_1 y} + E_{x_1}^- e^{jk_1 \sin\theta_1 y} = E_{x_2}^- e^{+jk_{y2} y} \quad .$$

This requires that $k_1 \sin\theta_1 = k_{y2}$, which is real, and then $k_{z2} = \sqrt{k_2^2 - k_{y2}^2}$. Thus we have waves propagating in the $+y$ direction and the $-z$ direction. The $+y$ directed wave is unattenuated, while the $-z$ wave is attenuated as

$$e^{jk_{z2}z} = e^{j(\beta - j\alpha)z} \quad ,$$

where

$$k_{z2} = [\omega^2 \mu_0 \epsilon_2 - k_1^2 \sin^2\theta_1]^{1/2} = k_1[\epsilon' - j\epsilon'' - \sin^2\theta_1]^{1/2} \quad .$$

We can solve for the attenuation, α, arriving at

$$\alpha = \frac{k_1 \sqrt{\epsilon'}}{\sqrt{2}} \left[\sqrt{\left(1 - \frac{\sin^2\theta_1}{\epsilon'}\right)^2 + \left(\frac{\epsilon''}{\epsilon'}\right)^2} - \left(1 - \frac{\sin^2\theta_1}{\epsilon'}\right) \right]^{1/2} \quad .$$

Thus, the one-way power attenuation through a forest of height h (meters) is

$$\text{ATTEN} = -8.686 \, \alpha \, h \, \text{dB} \quad .$$

It is obvious that for a fixed conductivity and fixed real part to the dielectric constant, ϵ', that as the frequency increases ϵ''/ϵ' approaches zero. Thus for ω large enough

$$\left(\frac{\epsilon''}{\epsilon'}\right)^2 \ll \left(1 - \frac{\sin^2\theta_1}{\epsilon'}\right)^2$$

and we can write

$$\alpha = \frac{k_1 \epsilon''}{2} \frac{1}{\sqrt{\epsilon' - \sin^2\theta_1}} = \frac{\eta_0 \sigma}{2} \frac{1}{\sqrt{\epsilon' - \sin^2\theta_1}} \quad \text{nepers/m} \quad , \tag{1}$$

which is seen to be independent of frequency. At some sufficiently large frequency and normal incidence

11

$$\alpha = \frac{\eta_0 \sigma}{2\sqrt{\epsilon'}} \text{ nepers/m} \qquad \eta_0 = 377 \text{ ohms} \quad .$$

At some sufficiently small frequency $\epsilon'' = \frac{\sigma}{\omega \epsilon_0} \gg \epsilon' - \sin^2 \theta_1 = \epsilon' - \cos^2 \phi_1$, where ϕ_1 is called the grazing angle. Then

$$\alpha = \frac{\omega \sqrt{\mu_0 \epsilon_0}}{\sqrt{2}} \left[\sqrt{(\epsilon' - \cos^2 \phi_1)^2 + \epsilon''^2} - (\epsilon' - \cos^2 \phi_1) \right]^{1/2}$$

$$\approx \omega \sqrt{\frac{\mu_0 \epsilon_0 \epsilon''}{2}} = \sqrt{\frac{\omega \mu_0 \sigma}{2}} = \sqrt{\pi f \mu_0 \sigma} \quad . \tag{2}$$

The latter is the form for attenuation of a plane wave in a conducting medium, as given by Ramo, Whinnery, and Van Duzer.[7] This form also holds if $\epsilon' = 1$ and $\phi = 0^\circ$.

Equations (1) and (2) suggest that the attenuation can be written as

$$\alpha = \text{constant} \times f^{0.5} \text{ dB/m}$$

over some frequency range, after which it transitions to a constant value.

This critical frequency can be found as follows: The constant attenuation condition applies when

$$\left(\frac{\sigma}{\omega \epsilon_0 \epsilon'} \right)^2 = \left(\frac{\epsilon''}{\epsilon'} \right)^2 \ll \left(\frac{\epsilon' - \cos^2 \phi_1}{\epsilon'} \right)^2$$

or

$$f \gg \frac{\sigma}{2 \pi \epsilon_0 (\epsilon' - \cos^2 \phi_1)} = f_c \quad .$$

As the condition pertains to the square of f, $f \sim 10 f_c$ should yield the constant attenuation condition

7. Ramo, Whinnery, and Van Duzer (1965) Fields and Waves in Communication Electronics, John Wiley & Sons, N.Y.

$$\alpha = \frac{\eta_0 \sigma}{2} \; \frac{1}{\sqrt{\epsilon' - \cos^2 \phi_1}} \; .$$

For low frequencies,

$$\frac{\sigma}{\omega \epsilon_0} \gg \epsilon' - \cos^2 \phi_1$$

or

$$f \ll \frac{\sigma}{2 \pi \epsilon_0 (\epsilon' - \cos^2 \phi_1)} = f_c \; .$$

Again, $f \approx \frac{f_c}{10}$ should be sufficient for $\alpha = \sqrt{\pi f \mu_0 \sigma}$. Tamir[5] indicates that the range of values for ϵ' and σ should be less than the limits he used. These were, for frequencies between 50 MHz and 100 MHz, $1.05 < \epsilon' < 1.15$ and $0.05 < \sigma < 0.15$ mS/m. Lippman[8] used the following values, considered good at 2 MHz:

$$\epsilon' = \epsilon_0 \qquad 0.02 < \sigma < 0.05 \; \text{S/m} \; . \; .$$

Surgent[1] suggested that at 190 MHz

$$1.01 < \epsilon' < 1.1 \; .$$

It is hard to conclude that σ is constant with frequency from this sampling of data. However, we can make this assumption and proceed, as our intent is to derive total attenuation in foliage curves consistent with the values on Figures 1, 2, and/or 3. Therefore, assuming some representative dielectric constant values, let us observe the resulting values for α in dB/m for varying radar ranges and heights as presented on Figure 5. It is obvious that high dielectric constants reduce the forest path length and the resultant attenuation rate in foliage for a constant conductivity. Figure 5(e) most closely approximates Figure 3 in terms of the trend of the curves with frequency. The specific curve, however, could not be reproduced.

How can the curves of Figure 5 be compared to those of Figure 2? Figure 2 contains measured attenuation versus frequency and has no hint of a plateau on the

---

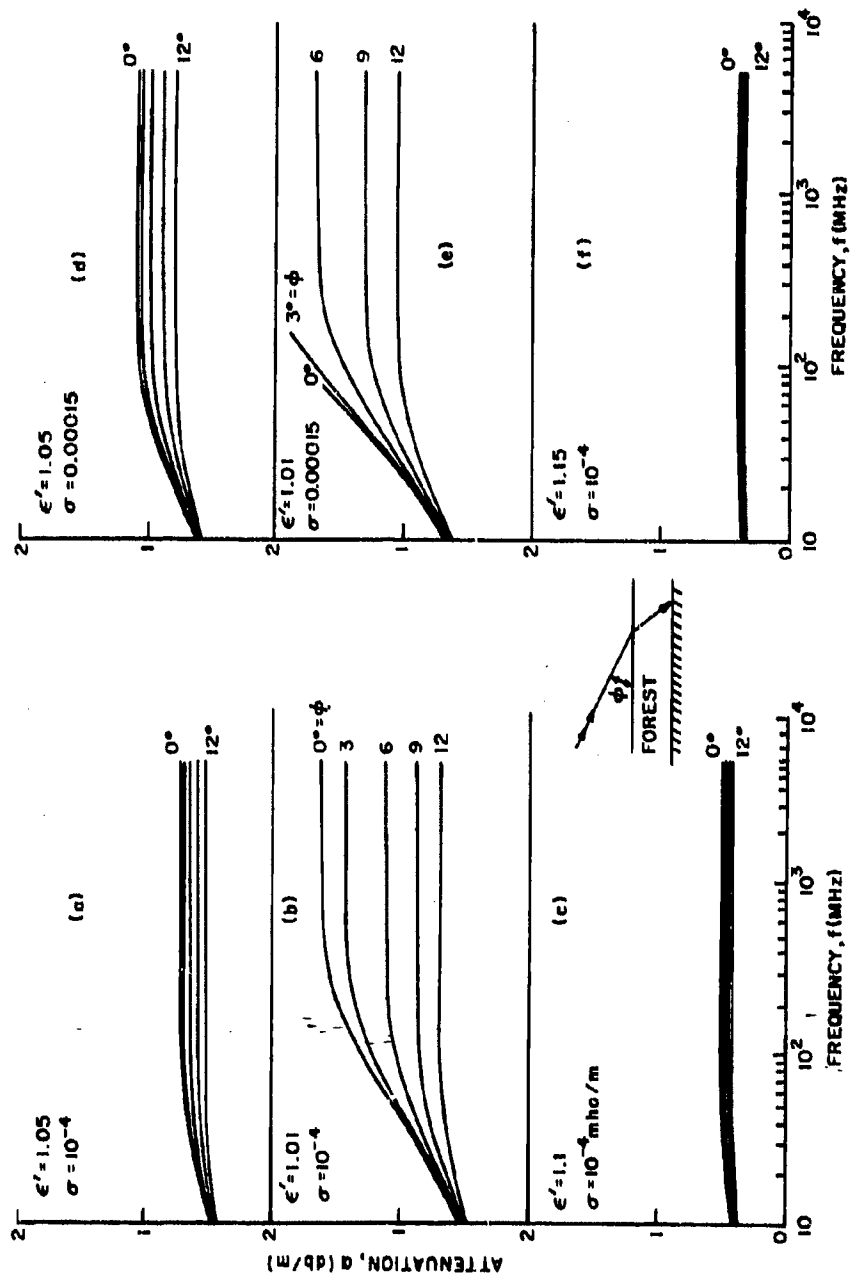8. Lippman, B.A. (1965) Jungle as a Communication Network, ARPA Report.

13

Figure 5. Foliage Attenuation per Unit of Forest Height vs Frequency — Constant Conductivity >10^{-4} S/m

14

attenuation. Figure 5 in turn is based upon an <u>assumption</u> of constant dielectric constant and conductivity with frequency. It was shown that for a sufficiently low frequency the attenuation can be written as

$$\alpha = 8.686 \sqrt{\pi \mu_0 \sigma} \ \sqrt{f} \ \ dB/m \quad . \tag{3}$$

This form agrees well with measured rates, with the frequency dependency varying from $\log_{10} f^{0.3}$ to $\log_{10} f^{3/4}$. However, this form for the attenuation should be good only for frequencies well below 1.8 MHz, as this is the previously defined critical frequency for values of $\sigma = 10^{-4}$ S/m and $\epsilon' = 1$. This critical frequency would suggest a constant value of α above 20 MHz, which is not supported by measurement.

Also, the attenuation would vary as

$$\alpha = 0.173 \sqrt{f_{MHz}} \ \ dB/m \quad ,$$

which doesn't agree with Figure 2 (that is, at 10 MHz, $\alpha = 0.55$ dB/m, not 0.01 dB/m).

To make Eq. (3) approximate the data of Figure 2 at 100 MHz, we must choose σ and ϵ' to be of the following orders of magnitude: $\epsilon' \approx 1.0$ and $\sigma \approx 1.6 \times 10^{-7}$ S/m. The latter quantity is 2 orders of magnitude below Tamir's smallest value. For various fixed conductivities in this range, curves of attenuation per meter of forest height are shown in Figure 6.

From Figures 5 and 6, it can be concluded that the constant complex conductivity with frequency model is incorrect.

A better model can be derived. The measured data of Figure 2 should hold for a wave in the forest that was generated at normal incidence. In this case,

$$\alpha = \frac{k_1 \sqrt{\epsilon'}}{\sqrt{2}} \left[\sqrt{1 + \left(\frac{\epsilon''}{\epsilon'}\right)^2} - 1 \right]^{1/2} \ \ neper/m \quad .$$

If we assume $\epsilon' =$ constant and $\epsilon''/\epsilon' \ll 1$, then

$$\alpha \approx \frac{\eta \sigma(\omega)}{2}$$

where $\eta =$ wave impedance in forest (real) $= \sqrt{\mu_0/\epsilon_0 \epsilon'} \approx 120\pi$ ohms. Then, using Nathanson's approximation[3] for the wave attention, we find
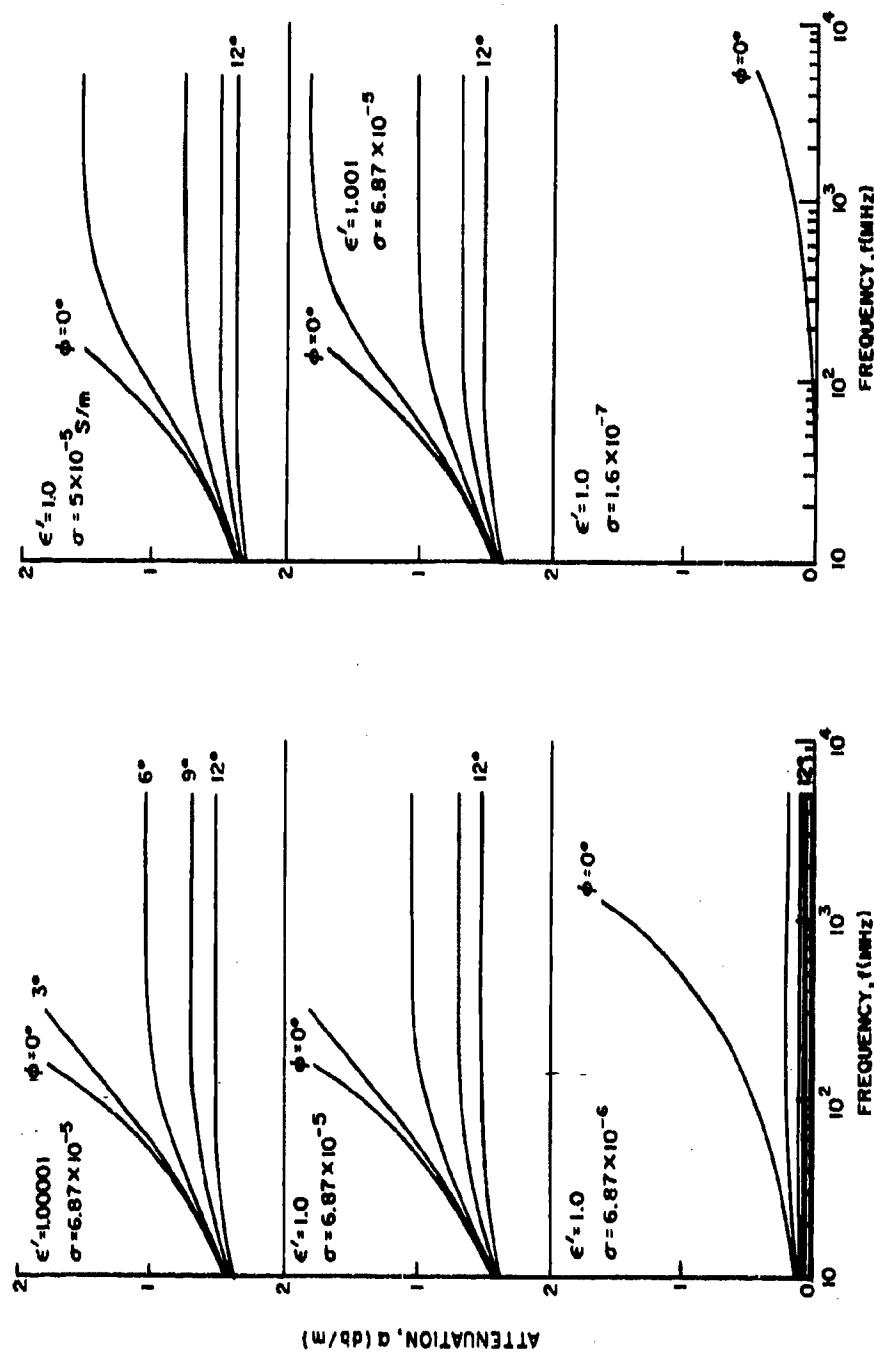
Figure 6. Foliage Attenuation per Unit of Forest Height vs Frequency — Constant Conductivity $<5 \times 10^{-5}$ S/m

16

$$\sigma(f) = \frac{2\alpha}{\eta_0} \sqrt{\epsilon'} = 0.86 \, f^{0.75} \, \mu S/m \; ; \; f \text{ in MHz} \; ; \; \epsilon' = 1 \quad .$$

It seems resonable then to use this variation in $\sigma(f)$ in evaluating the signal attenuation. This has been done, and the results are shown in Figures 7a through 7d.

These results are very much different from those obtained by using constant conductivity, but the results for normal incidence agree with measured data. In Figures 8, 9, and 10, these curves are plotted in log-log fashion to show their agreement with Figure 3. By design, the attenuation agrees at normal incidence with Nathanson's estimate. As the incidence angle departs from normal incidence (90°), the attenuation increases. This agrees with the model in which the attenuation per meter is constant at a given frequency, but the path length changes with incidence angle. Since at near-zero-degrees incidence the propagation constant k is nearly parallel to the dielectric surface, and the component of k parallel to this interface is real, all the attenuation must be absorbed by the propagation factor normal to the dielectric interface, k_z.

A physical model to explain this assumed variation of conductivity is as follows: The forest is filled with one type of material of constant conductivity and permittivity. However, this material is formed into numerous, assorted, rod-shaped bodies of various lengths, diameters, and length-to-diameter aspect ratios. Also, far more space is filled with twig and branch-size objects than is filled with trunk-size objects. This variation in density of object size results in a greater current density being produced at higher frequencies via there being more resonant objects at the higher frequencies. Of course, greater current density implies a higher conductivity, and greater attenuation over a given path length.

If the above is true, the difference between 400 and 1000 MHz at 3° incidence is 5.6 dB/m vs 1.2 dB/m one-way attenuation ($\epsilon' = 1.05$).

Queries were made to locate substantiation of Figure 3 at RADC and Lincoln Laboratories, but no originator could be found. It is thus advisable to use Figure 9 as a more realistic estimate of attenuation in foliage. Figure 9 is selected over Figures 8 and 10 as a dielectric constant of 1.05 is more consistent with Tamir[5] and Surgent's[1] conclusions.
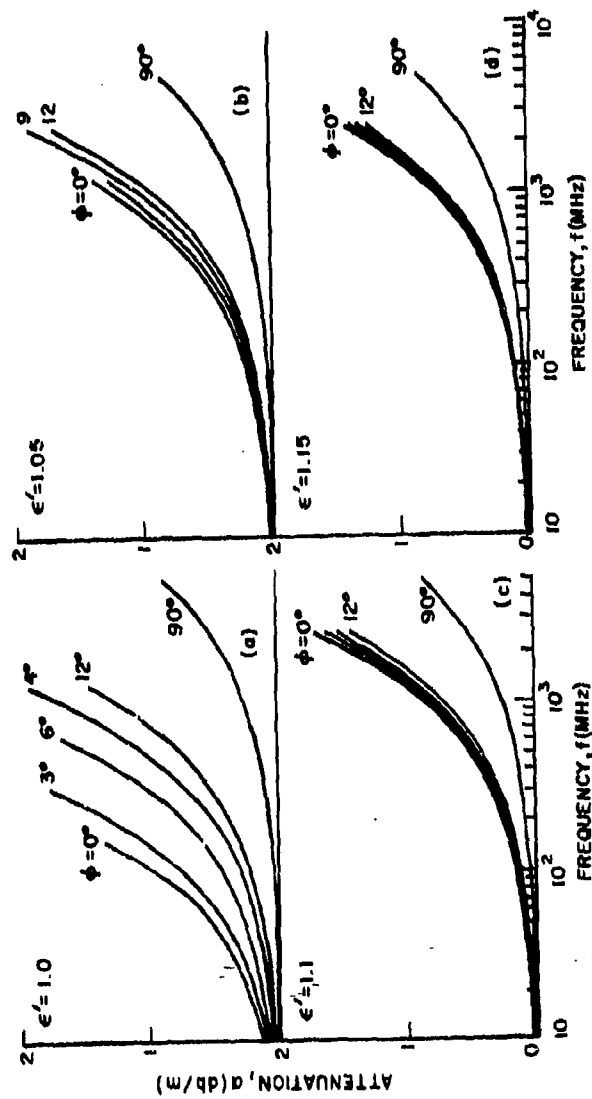
17

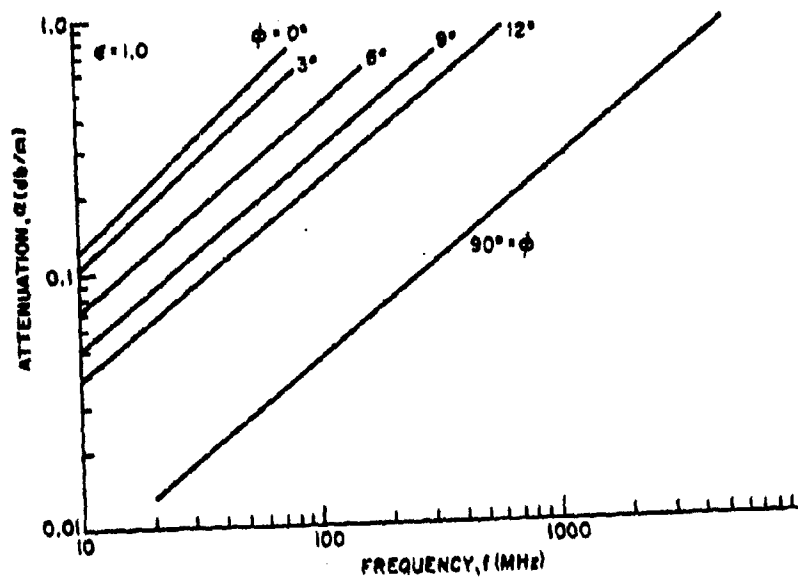Figure 7. Foliage Attenuation per Unit of Forest Height vs Frequency – Variable Conductivity

Figure 8. Foliage Attenuation per Unit of Forest Height vs Frequency —
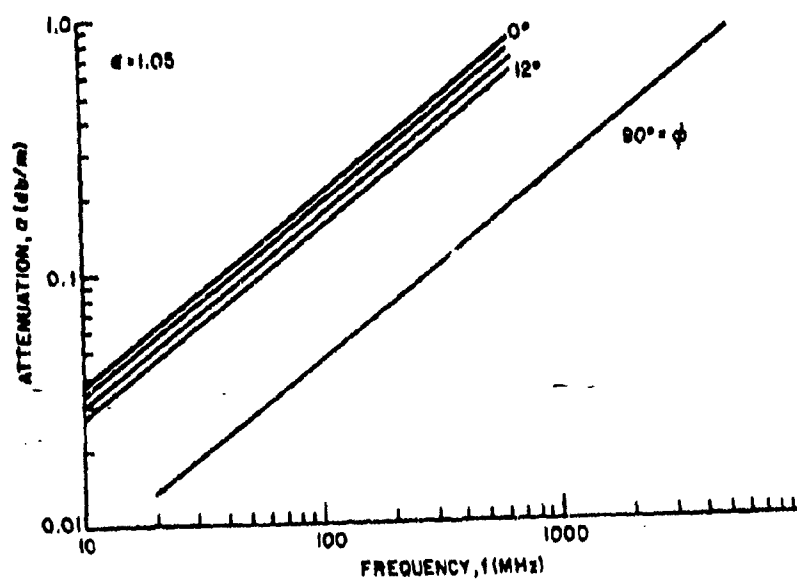Variable Conductivity $\epsilon = 1.0$

Figure 9. Foliage Attenuation per Unit of Forest Height vs Frequency —
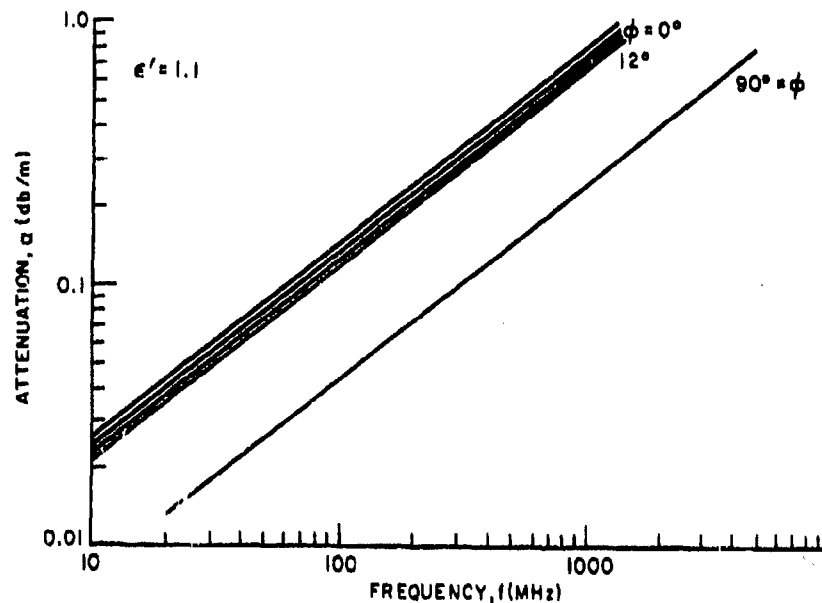Variable Conductivity $\epsilon = 1.05$

19

Figure 10. Foliage Attenuation per Unit of Forest Height vs Frequency —
Variable Conductivity $\epsilon = 1.1$

4. TRANSMISSION COEFFICIENT FORMULATION

Foliage attenuation, however, is not the only contributor to signal loss. At the smaller grazing angles, ϕ_1, a significant portion of the incident energy is re-flected from the dielectric discontinuity. The relationship governing the transmission into and reflection from the forest-air interface will be developed next.

For our horizontally polarized electric field, again from Figure 4, the fields must satisfy the following conditions at the boundary of regions I and II:

$$E_{x_1}^- + E_{x_1}^+ = E_{x_2}^- \quad , \quad H_{y_1}^- + H_{y_1}^+ = H_{y_2}^- \quad ,$$

that is, continuity of fields at the boundary.

If the fields in the two regions can be defined as planar with a real or complex propagation constant (e^{jk_z} as field travelling in -z direction),

$$\vec{E} = E_x \hat{x} = E_o \hat{x} e^{j\vec{k} \cdot \vec{r}} \quad , \quad \vec{k} = (\beta - j\alpha)\hat{k} \quad , \quad E_x = E_o e^{j(k_y y + k_z z)} \quad .$$

20

Then from

$$\nabla \times \vec{E} = -j\omega\mu_o \vec{H} = \begin{vmatrix} \hat{x} & \hat{y} & \hat{z} \\ \frac{\partial}{\partial x} & \frac{\partial}{\partial y} & \frac{\partial}{\partial z} \\ E_x & 0 & 0 \end{vmatrix} = \hat{y}\,\frac{\partial}{\partial z}\,E_x + \hat{z}\,\left(-\frac{\partial}{\partial y}\,E_x\right)$$

$$= j\,E_x(k_z\hat{y} - k_y\hat{z}) \quad .$$

In region I for the incident field

$$\frac{E_{x_1}^-}{H_{y_1}^-} = -\frac{\omega\mu_o}{k_{z1}} \quad , \qquad \frac{E_{x_1}^-}{H_{z_1}^-} = \frac{\omega\mu_o}{k_{y_1}}$$

and for the reflected field

$$\frac{E_{x_1}^+}{H_{y_1}^+} = \frac{\omega\mu_o}{k_{z_1}} \quad .$$

Similarly, in region II

$$\frac{E_{x_2}^-}{H_{y_2}^-} = -\frac{\omega\mu_o}{k_{z_2}}$$

Inserting these ratios into the boundary conditions yields

$$\left|\frac{E_{x_2}^-}{E_{x_1}^-}\right| = \left|\frac{2k_{z_1}}{k_{z_1} + k_{z_2}}\right| = \tau = \text{transmission coefficient} \quad .$$

As

$$k_{z_2} = \sqrt{k_2^2 - k_{y_2}^2} \quad , \quad k_{y_2} = k_{y_1} = k_1 \sin\theta_1 \quad , \quad k_{z_1} = k_1 \cos\theta_1$$

and

$$k_2^2 = \omega^2 \mu_0 \epsilon_0(\epsilon' - j\epsilon'') = k_1^2(\epsilon' - j\epsilon'') \quad .$$

we have

$$\left| \frac{E_{x_2}^-}{E_{x_1}^-} \right| = \tau = \left| \frac{2 \cos \theta_1}{\cos \theta_1 + \sqrt{\epsilon' - j\epsilon'' - \sin^2 \theta_1}} \right| \quad .$$

If we allow $\theta_1 \to \pi/2$, $\tau \to 0$ unless $\epsilon' - j\epsilon'' - \sin^2 \theta_1 \to 0$ properly. But this cannot be if $\epsilon'' \neq 0$. Thus, for either $\epsilon' > 1$ or $\epsilon'' \neq 0$, as grazing incidence is approached the transmission into medium two goes to zero. This loss must be added to the actual attenuation in medium two.

The incident power in region I is given by

$$P_1 = \left| \frac{1}{2} \operatorname{Re} (E \times H^*) \right| = \left| E_{x_1}^- \right|^2 / 2\eta_1 \quad .$$

The power flowing through region II at the interface is

$$P_2 = \left| \frac{1}{2} \operatorname{Re} (E_2 \times H_2^*) \right| \quad .$$

As

$$H_2 = H_y \hat{y} + H_z \hat{z} = \frac{E_{x_2}^-}{\omega \mu_0} (-k_{z_2} \hat{y} + k_{y_2} \hat{z}) \quad ,$$

we can write

$$E_2 \times H_2^* = E_{x_2}^- \hat{x} \times \frac{E_{x_2}^{-*}}{\omega \mu_0} (-k_{z_2}^* \hat{y} + k_{y_2}^* \hat{z})$$

$$= - \frac{\left| E_{x_2}^- \right|^2}{\omega \mu_0} (k_{z_2}^* \hat{z} + k_{y_2}^* \hat{y}) = - \frac{\left| E_{x_2}^- \right|^2}{\omega \mu_0} \vec{k}_2^* \quad .$$

22

Then

$$P_2 = \left| -\frac{\left|E_{x_2}^-\right|^2}{2\omega\mu_o}\ \mathrm{Re}\ (\vec{k}_2^*) \right| = \frac{\left|E_{x_2}^-\right|^2}{2\omega\mu_o}\ \left|\mathrm{Re}\ (\vec{k}_2^*)\right|$$

with

$$\vec{k}_2 = k_{y_2}\ \hat{y} + (k_{z_{2R}} + jk_{z_{2I}})\ \hat{z}$$

$$P_2 = \frac{\left|E_{x_2}^-\right|^2}{2\omega\mu_o}\ \sqrt{k_{y_2}^2 + k_{z_{2R}}^2}\ .$$

As

$$k_{y_2} = k_1 \sin\theta_1$$

$$k_{z_2} = k_1 \sqrt{\epsilon' - \cos^2\phi_1 - j\epsilon''}\ ,$$

the real part of k_{z_2} is

$$k_{z_{2R}} = \frac{k_1}{\sqrt{2}}\left[\epsilon' - \cos^2\phi_1 + \sqrt{(\epsilon' - \cos^2\phi_1)^2 + \epsilon''^2}\right]^{1/2}$$

and

$$\frac{P_2}{P_1} = |\tau|^2\left[\cos^2\phi_1 + \frac{\epsilon' - \cos^2\phi_1 + \sqrt{(\epsilon' - \cos^2\phi_1)^2 + \epsilon''^2}}{2}\right]^{1/2}\ .$$

For small grazing angles, $\phi_1 \to 0$, what is the relative size of ϵ'' to $\epsilon' - \cos^2\phi_1$? Using the formulation for volume conductivity developed previously,

$$\sigma(f) = 0.272 \times 10^{-10}\ f^{3/4}\ \mathrm{S/m}$$

$$\epsilon'' = \frac{\sigma}{\omega\epsilon_o} \sim \frac{0.5}{f^{1/4}} \ll \epsilon' - \cos^2\phi_1 \quad \text{for all cases where } \epsilon' = 1.05\ .$$

Therefore

$$\frac{P_2}{P_1} = |\tau|^2 \sqrt{\epsilon'} \quad .$$

This transmission coefficient is plotted in Figure 11 for various values of dielectric constant and a variable conductivity. For the range of values chosen, it is obvious that the conductivity plays no role. If the conductivity is increased by a factor of 10, then the transmission coefficient is only weakly dependent upon frequency, as shown on Figure 12. This is due to $\epsilon'' = \frac{\sigma}{\omega\epsilon} \to 0$ as $\omega \to \infty$. For all cases it is obvious that for grazing angles less than 4°, the transmitted signal is severely attenuated; that is, $10 \log|\tau|^2 > 3$ dB, even at 13° grazing angle. It thus seems that overcoming the specular reflection from foliage requires a significant radar transmitter power increase.

If it is argued that both the conductivity and permittivity are constant with frequency, the percentage of power penetrating the foliage remains the same at frequencies above 100 MHz, as the transmission coefficient is relatively insensitive to the conductivity. In fact, using a $\sigma = 0.15$ mS/m, τ decreases for frequencies below 100 MHz, as shown in Figure 13.

In researching the subject of the fraction of the incident power that enters region II, I found another formulation for the transmission coefficient that has been utilized by others.[9] This formulation is

$$T = \frac{\sin 2\theta_1 \sin 2\theta_2}{\sin^2 (\theta_1 + \theta_2)} \quad ,$$

with θ_1 and θ_2 as defined in Figure 4. This equation was, in turn, extracted from Stratton.[10] A review of Stratton shows that this equation gives the fraction of power normally incident on region II that enters region II. This is not the same as the total power in region II relative to the total power incident from region I, as given by

$$T' = |\tau|^2 \sqrt{\epsilon} = \left| \frac{2 \cos \theta_1}{\cos \theta_1 + \sqrt{\epsilon' - j\epsilon'' - \sin^2 \theta_1}} \right|^2 \frac{\sin \theta_1}{\sin \theta_2} \quad .$$

9. Labitt, M. (1978) Visibility of Targets as Seen From a Long-Range Airborne Radar, Lincoln Lab Memo 43M-885.

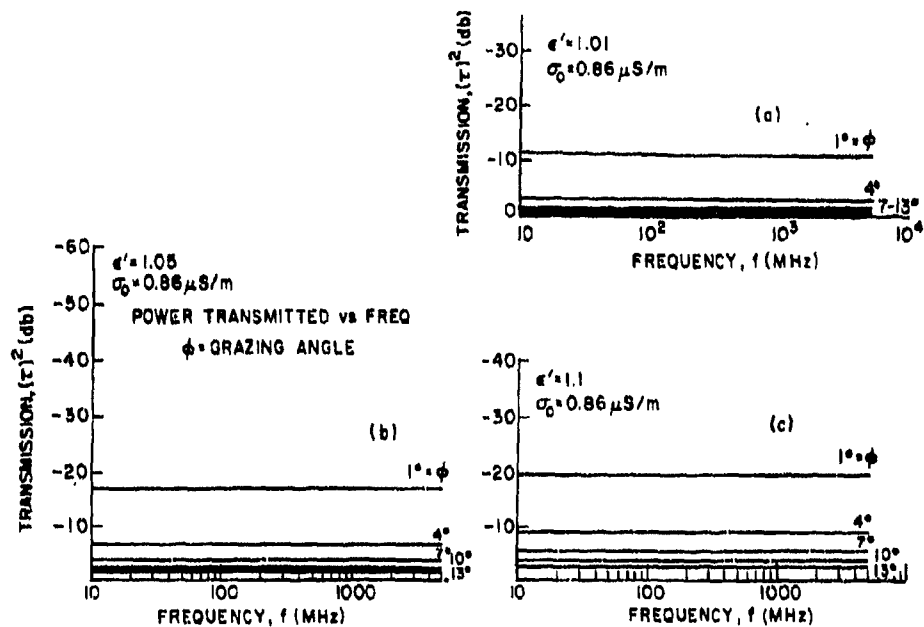10. Stratton, J.A. (1941) Electromagnetic Theory, p 496, McGraw Hill.

24

Figure 11. Foliage/Air Interface Transmission Coefficient vs Frequency -- Normal Conductivity
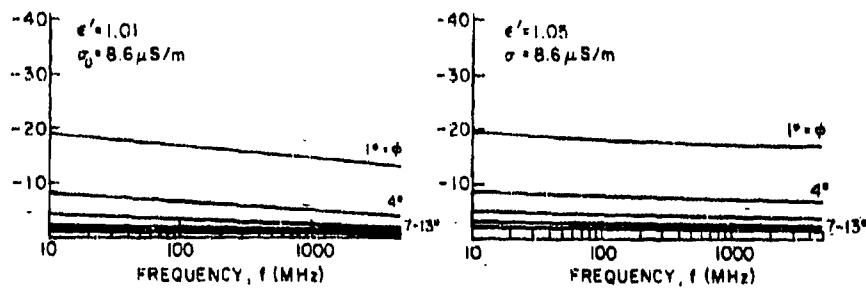

Figure 12. Foliage/Air Interface Transmission Coefficient vs Frequency -- Increased Conductivity
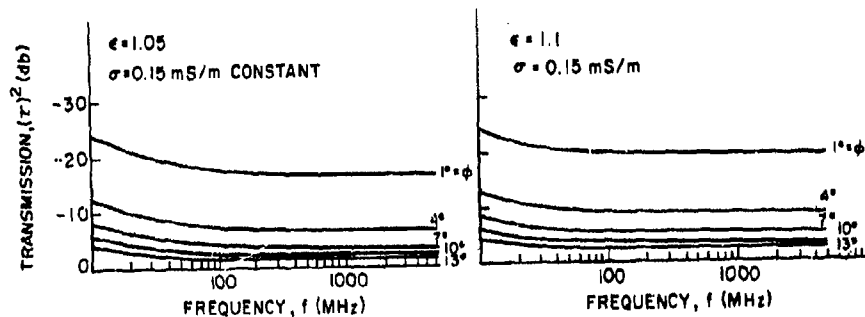
26

Figure 13. Foliage/Air Interface Transmission Coefficient vs Frequency —
Constant Conductivity

If $\epsilon'' = 0$, we can write

$$T' = \frac{\sin 2\theta_1 \; 2\cos \theta_1 \sin \theta_2}{\sin^2 (\theta_1 + \theta_2)}$$

and the results differ by

$$\frac{T'}{T} = \frac{\cos \theta_1}{\cos \theta_2} = \frac{\sin \phi_1}{\sin \phi_2} \quad .$$

Thus at small grazing angles, a larger transmission loss is calculated herein
than that derived in Labitt.[9]

Combining now the transmission loss and the attenuation loss we can derive
the two-way signal loss experienced by an AMT1 radar looking for targets under a
foliage canopy. Of course, this excludes the other loss mechanisms previously
mentioned. Choosing for parameter $\epsilon' = 1.05$, $\sigma = 0.86 \; \mu S/m$ at 1 MHz, and a
forest height of 50 ft (15.24 m), the results are as tabulated in Table 1.

Table 1. Total Foliage Attenuation Example

ϕ_1	Freq, GHz	α dB/m	$\|\tau\|^2$	Total Atten, dB
4°	0.4 1.0	0.56 1.2	7 7	31.1 50.6
12°	0.4 1.0	0.42 0.8	2 2	16.8 28.4

26

References

1. Surgent, L. V. (1974) Foliage Penetration Radar: History and Development Technology, Army Land Warfare Lab, Aberdeen Proving Ground, Md.

2. Chudleigh, W., Moulton, S. (1973) Long-Range Standoff Radar Surveillance Study, AFCRL-TR-73-0145.

3. Nathanson, F. E. (1969) Radar Design Principles, McGraw Hill, p 19.

4. Lincoln Laboratory (1969) TR 472, pp 92-93.

5. Tamir, T. (1967) On radio-wave propagation in forest environments, APS-15 (No. 6).

6. Lincoln Laboratory (1969) Tactical Radar Program, ESD-TR-69-354, Quarterly Progress Report.

7. Ramo, Whinnery, and Van Duzer (1965) Fields and Waves in Communication Electronics, John Wiley & Sons, N. Y.

8. Lippman, B. A. (1965) Jungle as a Communication Network, ARPA Report.

9. Labitt, M. (1976) Visibility of Targets as Seen From a Long-Range Airborne Radar, Lincoln Lab Memo 43M-885.

10. Stratton, J. A. (1941) Electromagnetic Theory, p 496, McGraw Hill.

MISSION
of
Rome Air Development Center

RADC plans and conducts research, exploratory and advanced development programs in command, control, and communications (C^3) activities, and in the C^3 areas of information sciences and intelligence. The principal technical mission areas are communications, electromagnetic guidance and control, surveillance of ground and aerospace objects, intelligence data collection and handling, information system technology, ionospheric propagation, solid state sciences, microwave physics and electronic reliability, maintainability and compatibility.

Best Available Copy